# Turbulent superstructures in Rayleigh-Bénard convection

Jörg Schumacher
Technische Universität Ilmenau
Germany

Martin Ender (TU München)
Kathrin Padberg-Gehle (Leuphana Universität Lüneburg)
Ambrish Pandey (TU Ilmenau)
Janet D. Scheel (Occidental College Los Angeles)
Christiane Schneide (Leuphana Universität Lüneburg)
Rüdiger Westermann (TU München)

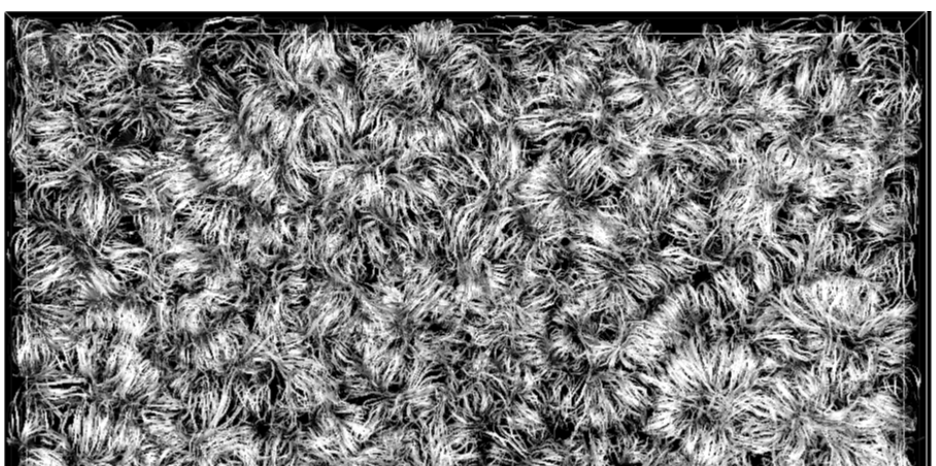

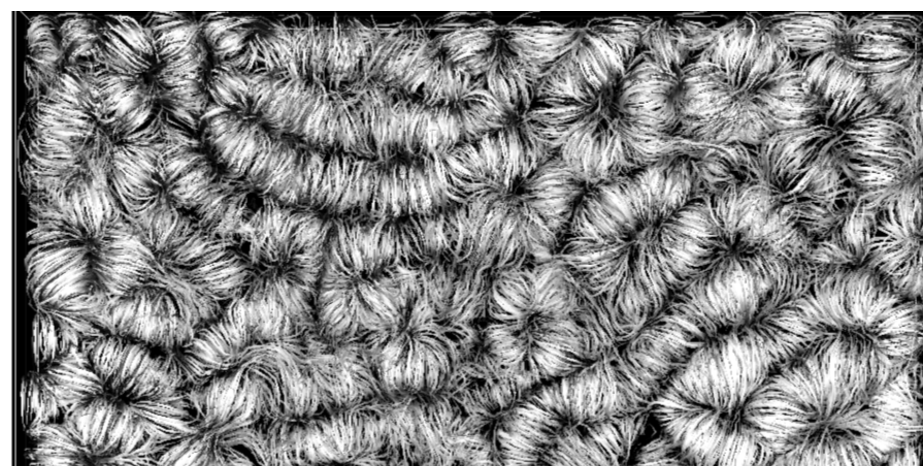

# Turbulent convection in nature

## Solar Granulation & Supergranulation

$$Ra \gtrsim 10^{22} \quad Pr \lesssim 10^{-3}$$

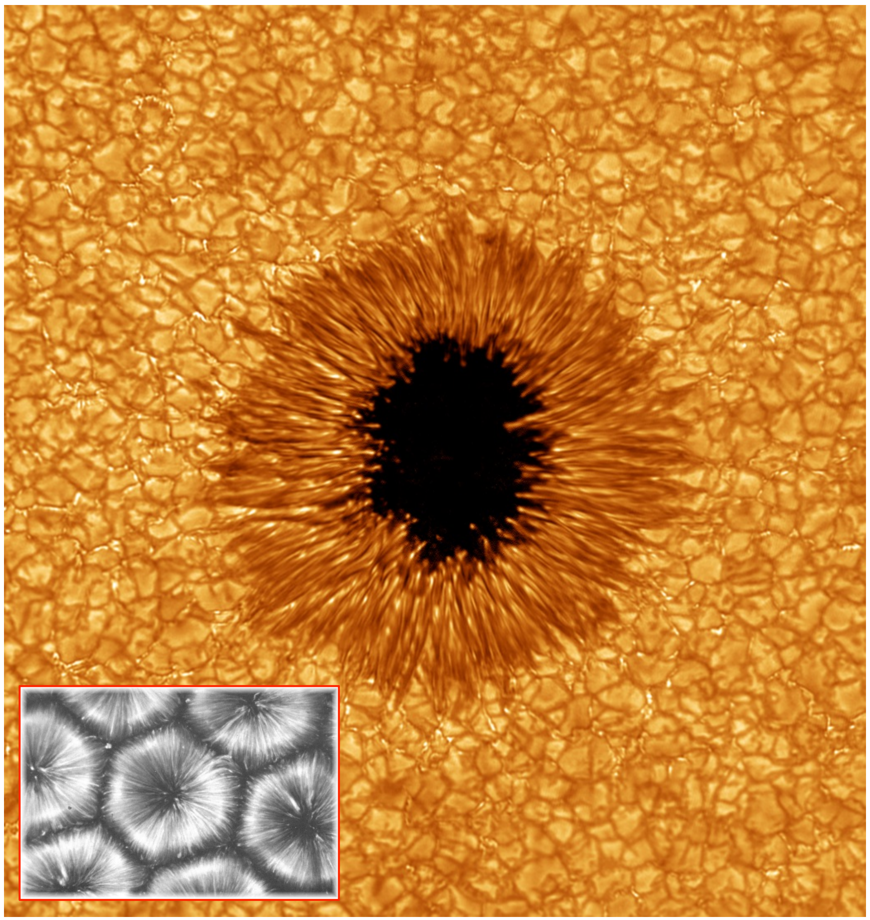

Big Bear Solar Observatory

## Cloud Streets over the Bering Sea

$$Ra \sim 10^{18} \quad Pr = 0.7$$

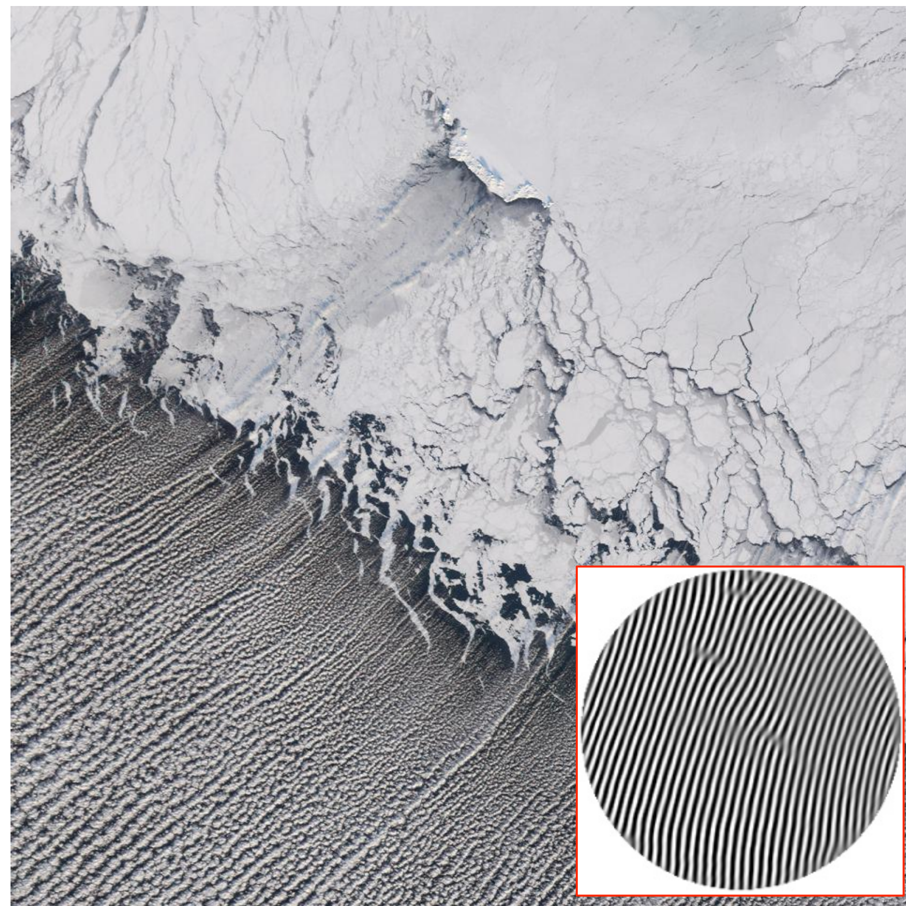

NASA Modis Mission

# Questions

- Do large-scale patterns exist in turbulent Rayleigh-Bénard convection (RBC)?
- Are these patterns relics from the onset or the weakly nonlinear regime of RBC?
- What are the typical spatial and temporal scales of these patterns and how do they depend on Ra and Pr?
- Are the pattern scales related to the boundary layer dynamics?
- Can we develop simplified models for the large-scale patterns?
- What is their role for turbulent transport?

# Numerical simulations

*Fischer, J. Comp. Phys. 1997; Emran, Scheel & JS, New J. Phys. 2013*

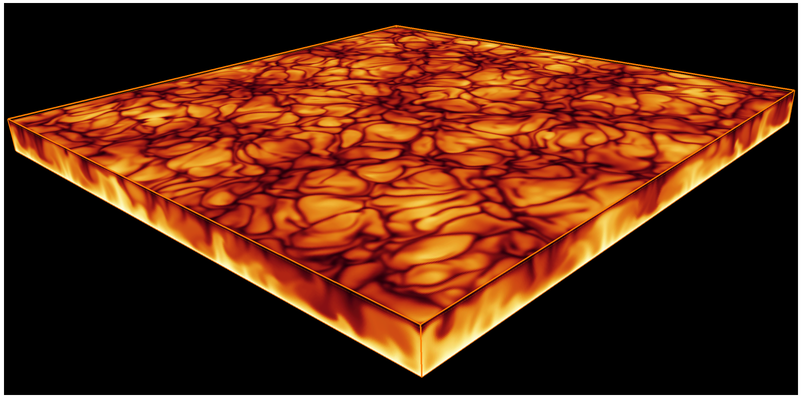

- 3d Boussinesq equations in closed rectangular cell
- 25:25:1
  $0.005 \leq Pr \leq 70$
  $2300 \leq Ra \leq 10^7$
- Spectral element method Nek5000
  Small-scale gradients at walls


# Instantaneous fields at Ra=$10^5$

Pr=0.021

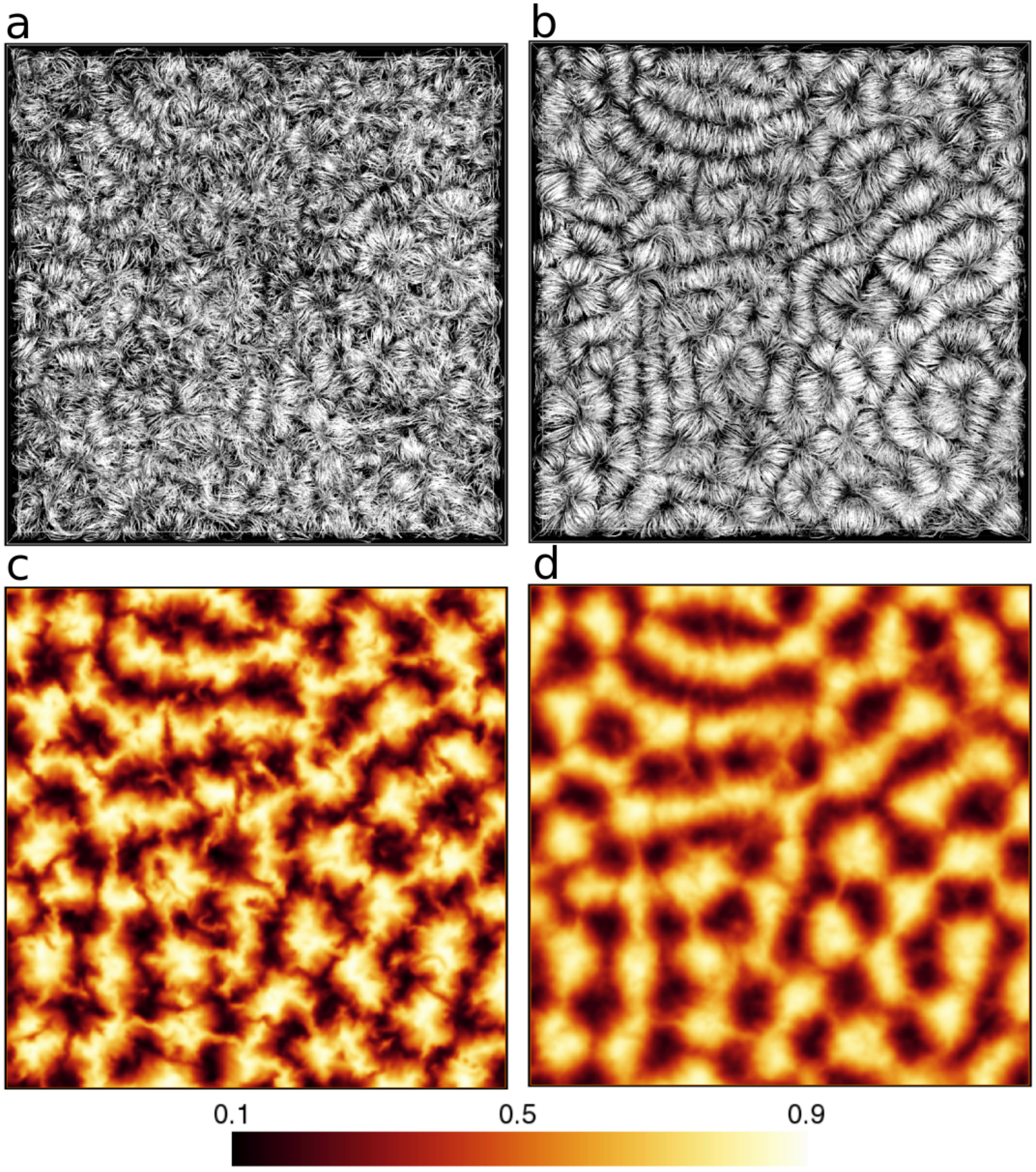

# Magnitude of superstructures

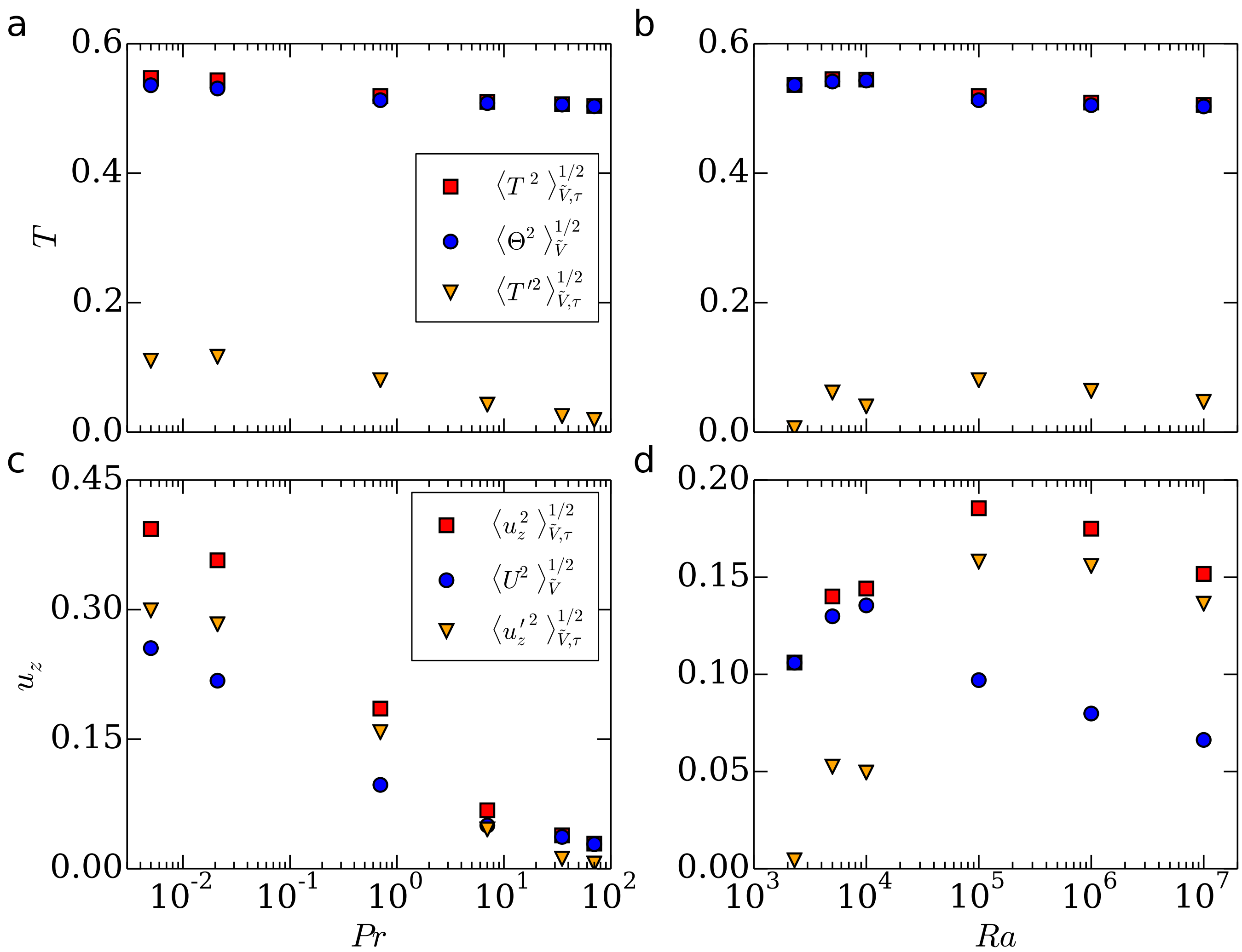


$$u_z(\boldsymbol{x},t) = U(\boldsymbol{x}) + u'_z(\boldsymbol{x},t)$$
$$T(\boldsymbol{x},t) = \Theta(\boldsymbol{x}) + T'(\boldsymbol{x},t)$$

# Time-averaged fields at $Ra=10^5$

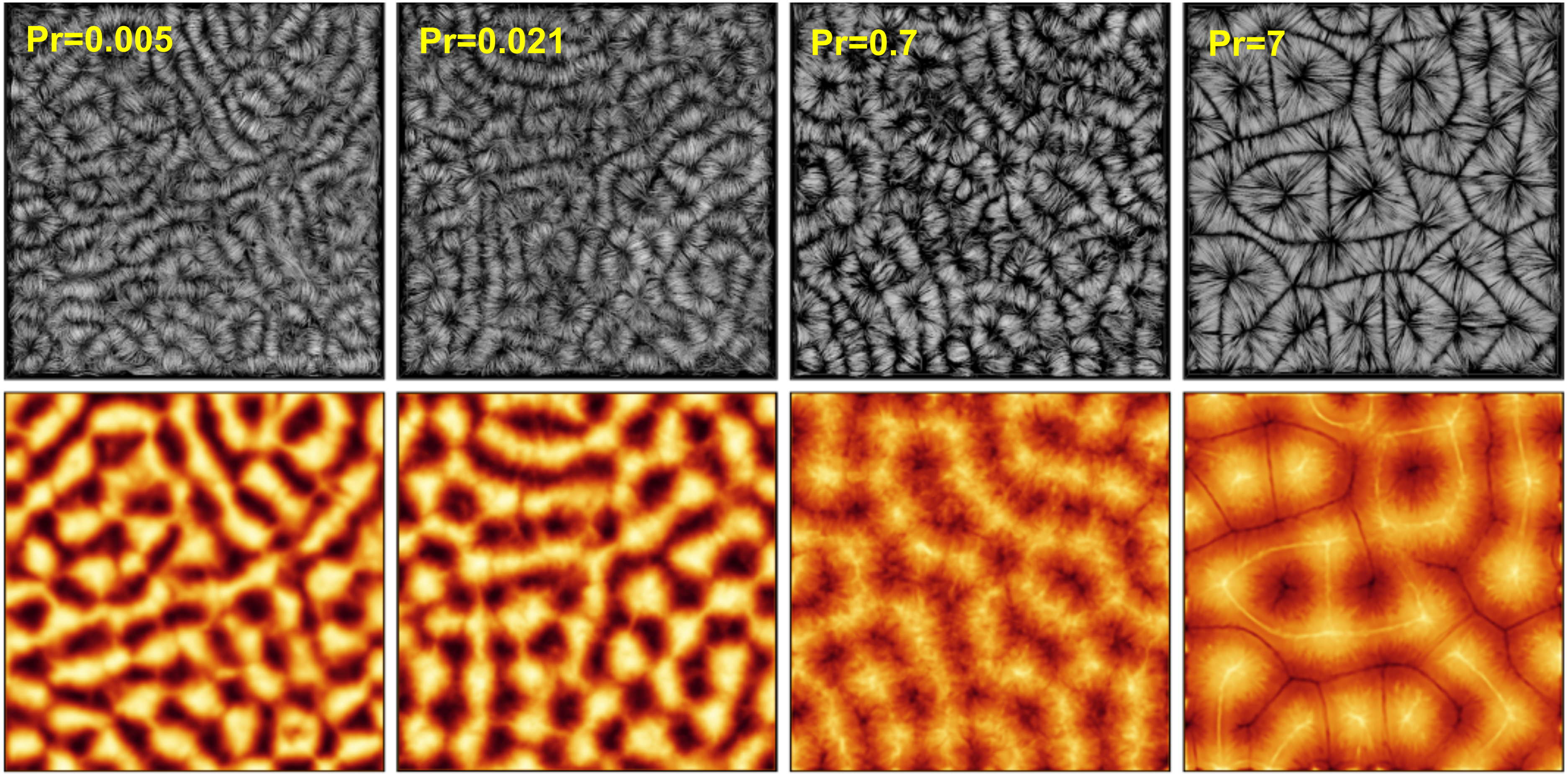


Regular patterns (= turbulent superstructures) are detected for all Pr

# Time-averaged fields at Pr=0.7

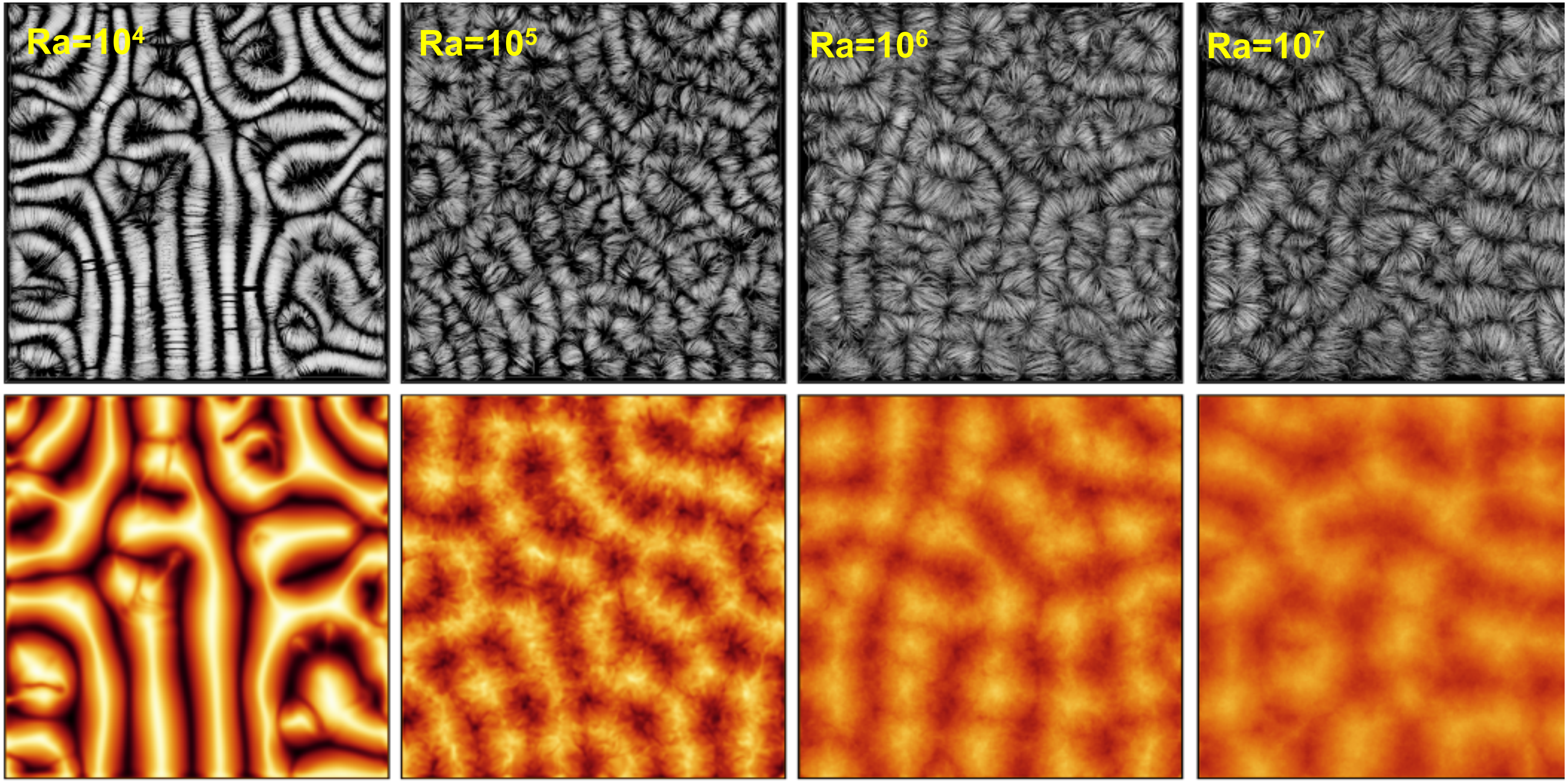


Regular patterns (= turbulent superstructures) are detected for all Ra

What are the typical scales and how do they depend on Ra, Pr?

# Scale separation

Fast & Small Scales | Slow & Large Scales

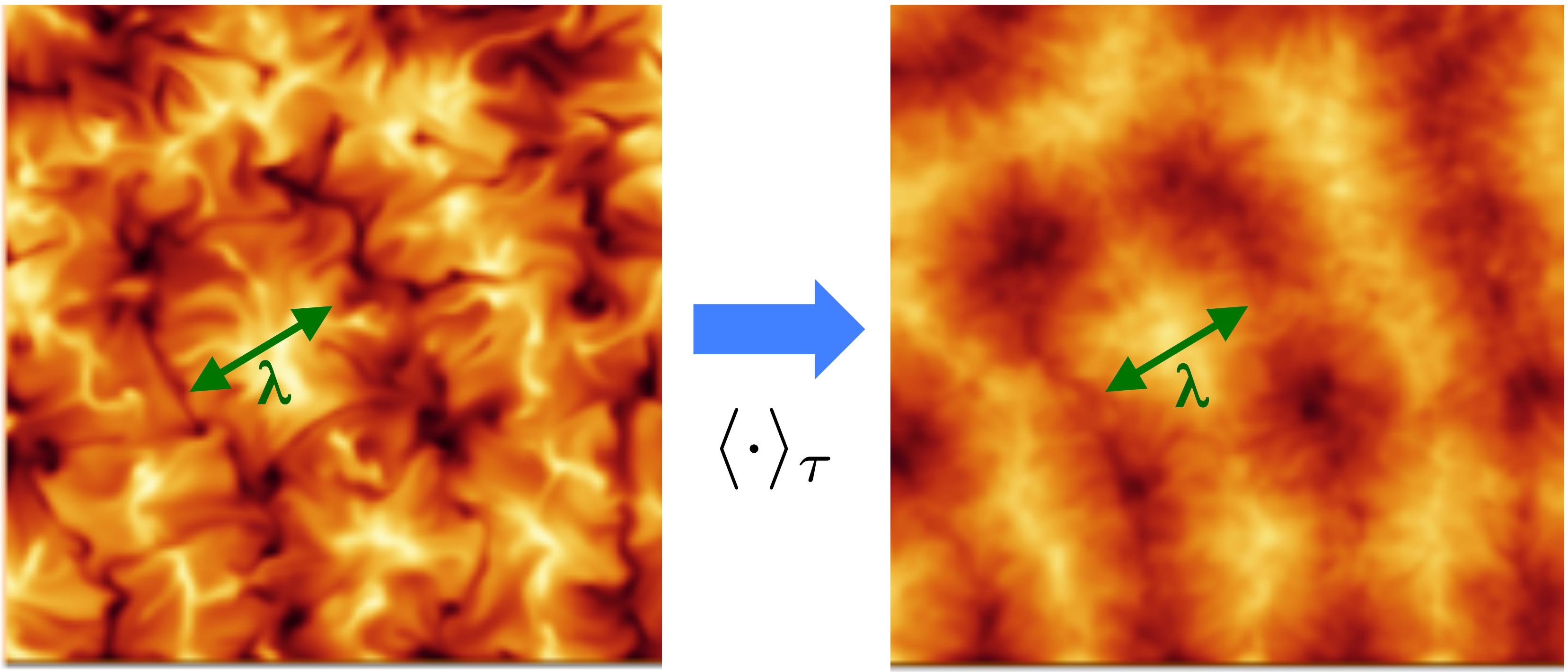


$t < \tau \quad \ell < \lambda$ | $t > \tau \quad \ell > \lambda$

$$U(x, y; \tau, t_0) = \frac{1}{\tau} \int_{t_0 - \tau/2}^{t_0 + \tau/2} u_z(x, y, z = 1/2, t')\, dt'$$

$$\Theta(x, y; \tau, t_0) = \frac{1}{\tau} \int_{t_0 - \tau/2}^{t_0 + \tau/2} \theta(x, y, z = 1/2, t')\, dt' .$$

# Time scales in RB convection

- Free-fall time $T_f = \frac{H}{U_f} = \frac{H}{\sqrt{g\alpha\Delta T H}}$
- Diffusion time $t_d = \frac{H^2}{\kappa} = \sqrt{RaPr}\,T_f$ $\longrightarrow$ $t_d^{\perp} = \frac{(\Gamma H)^2}{\kappa} = \Gamma^2 t_d$
- Viscous time $t_v = \frac{H^2}{\nu} = \sqrt{\frac{Ra}{Pr}}\,T_f$
- Lagrangian turnover time $10 - 20T_f$
  *(Emran & JS, Phys. Rev. E 2010)*

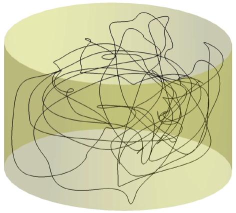

| Pr at Ra=$10^5$ | $T_f$ | $t_d$ | $t_v$ | $t_g = Ra^{1/2}\,T_f$ |
|---|---|---|---|---|
| 0.005 | 1 | 22 | 4472 | 316 |
| 0.021 | 1 | 46 | 2182 | 316 |
| 0.7 | 1 | 265 | 378 | 316 |
| 7 | 1 | 837 | 120 | 316 |
| 70 | 1 | 2646 | 38 | 316 |

# What is the appropriate time interval?

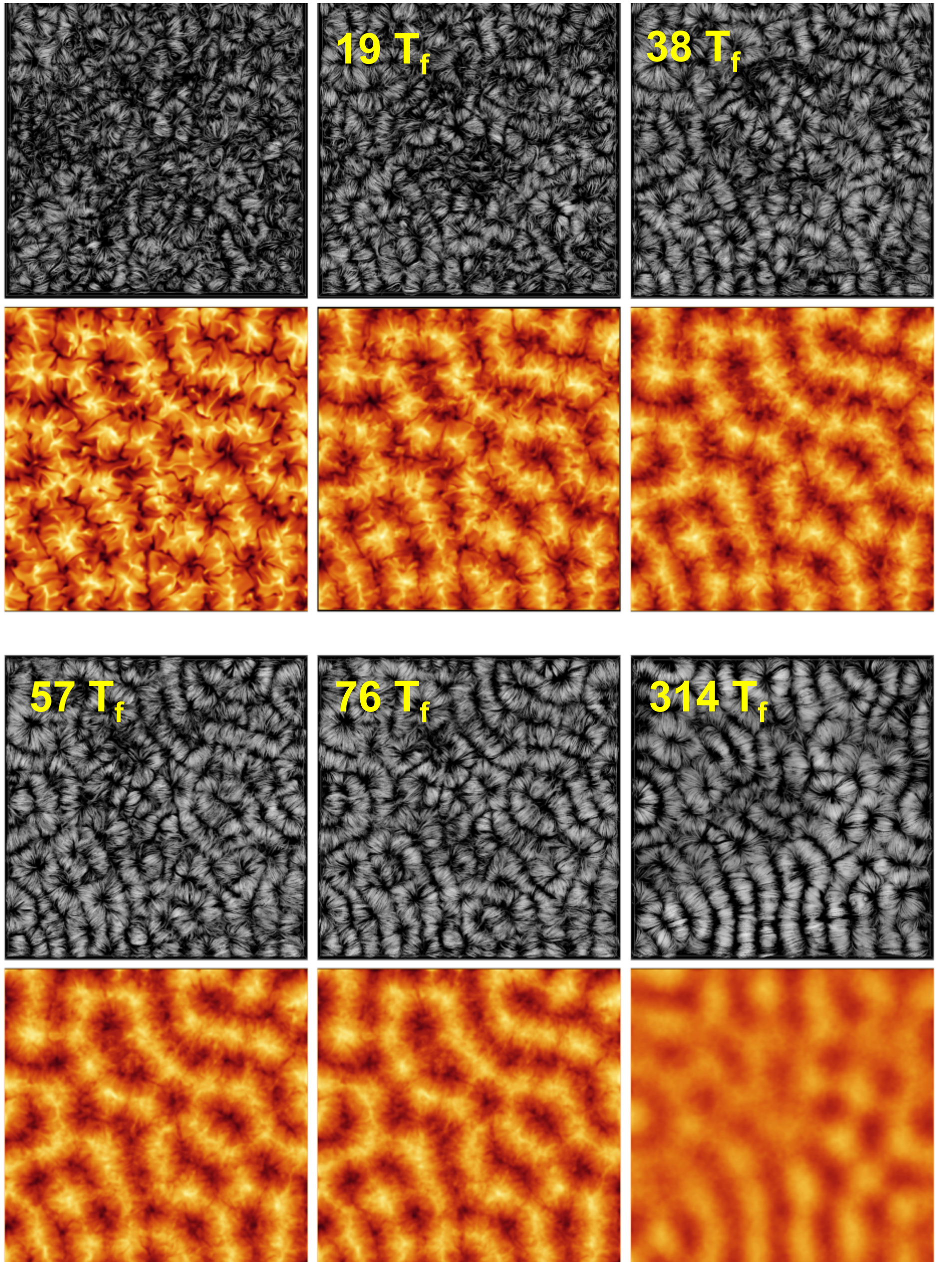


Mean turnover time τ in a superstructure roll

$$T_f \ll \tau \ll \max(t_v, t_d)$$

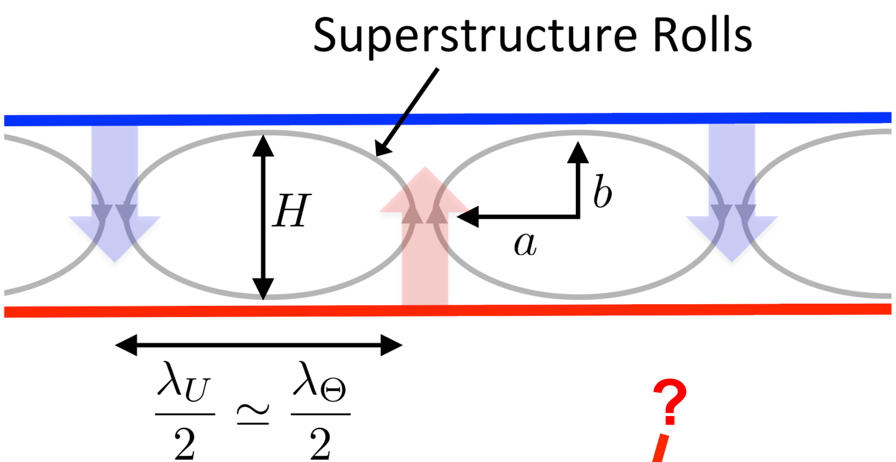


$$\tau(Ra, Pr) \sim \frac{\ell}{u_{rms}} = \frac{\pi\left(\frac{1}{4}\lambda_U + \frac{1}{2}H\right)}{\langle u_i^2 \rangle_{V,t}^{1/2}}$$

# Pattern scales of $u_z$ and θ in midplane

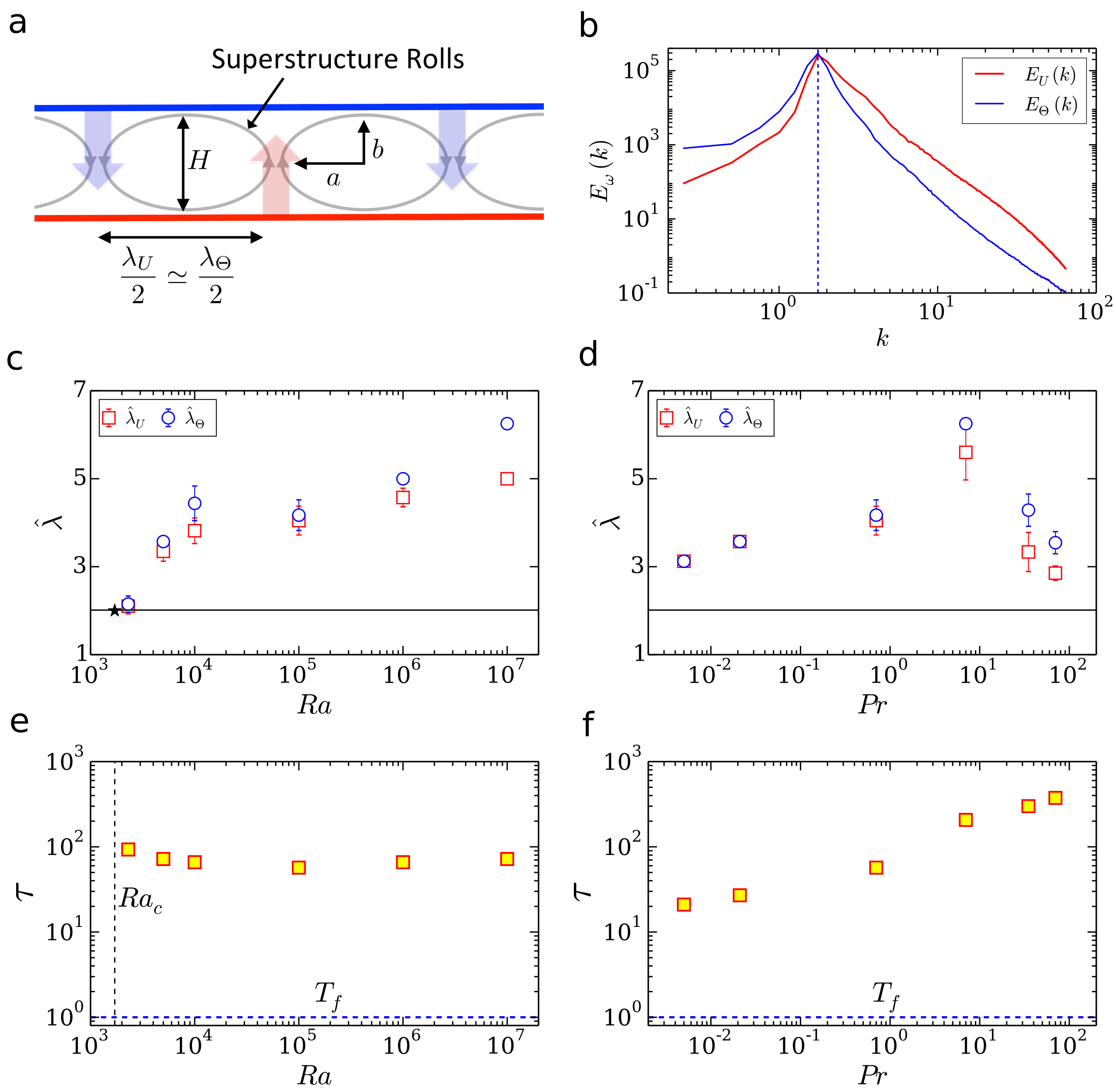

# Slow evolution of superstructures

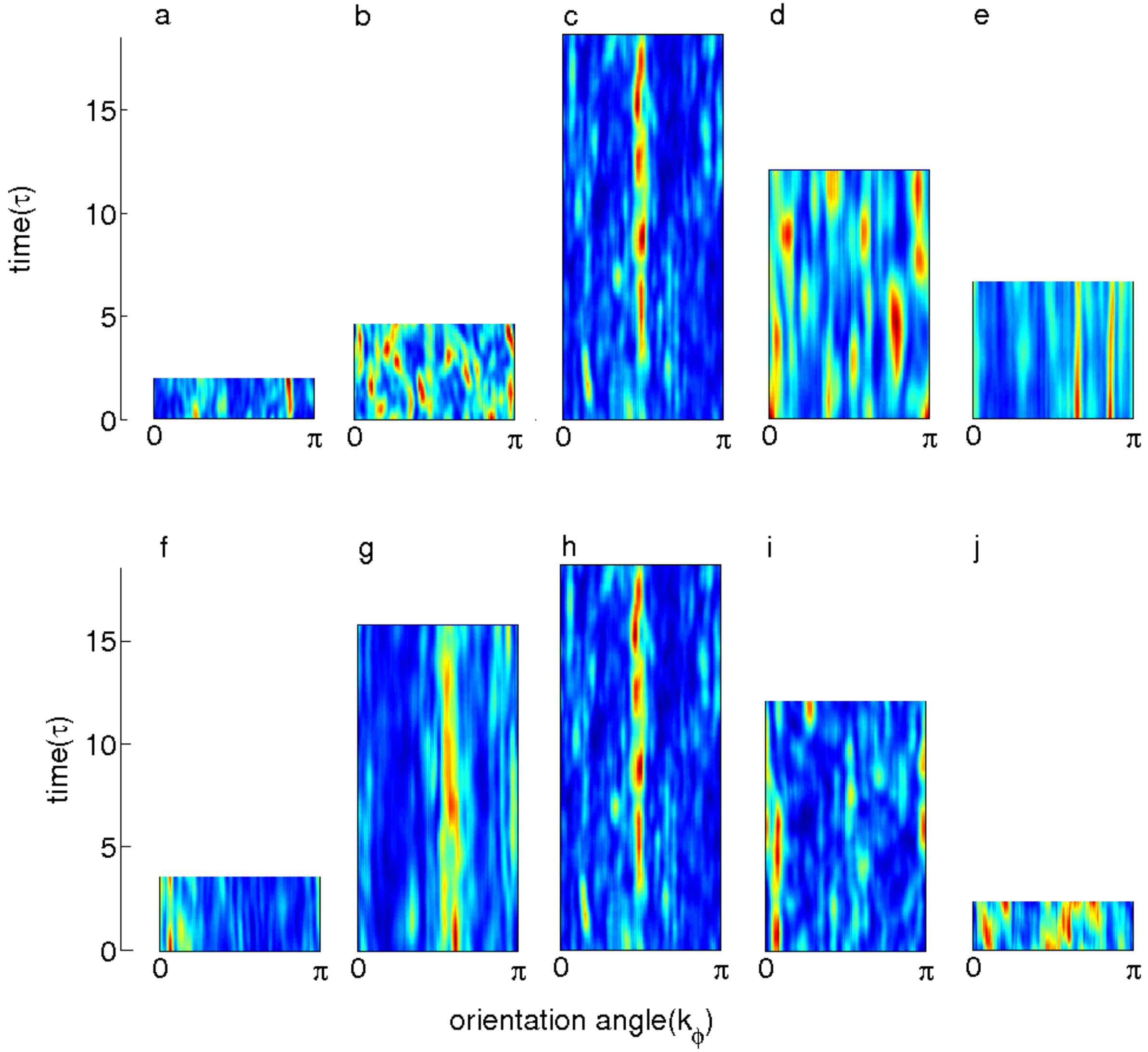


Pr=0.005
0.021
0.7
7
70

Ra=5000
$10^4$
$10^5$
$10^6$
$10^7$

$$E_\Theta(k_\phi;\tau,t_0) = \frac{1}{k_m}\int_0^{k_m} |\hat{\Theta}(k,k_\phi;\tau,t_0)|^2\, dk$$

# Busse balloon

*Busse, Rep. Prog. Phys. 1978; Cross & Hohenberg, Rev. Mod. Phys. 1993*

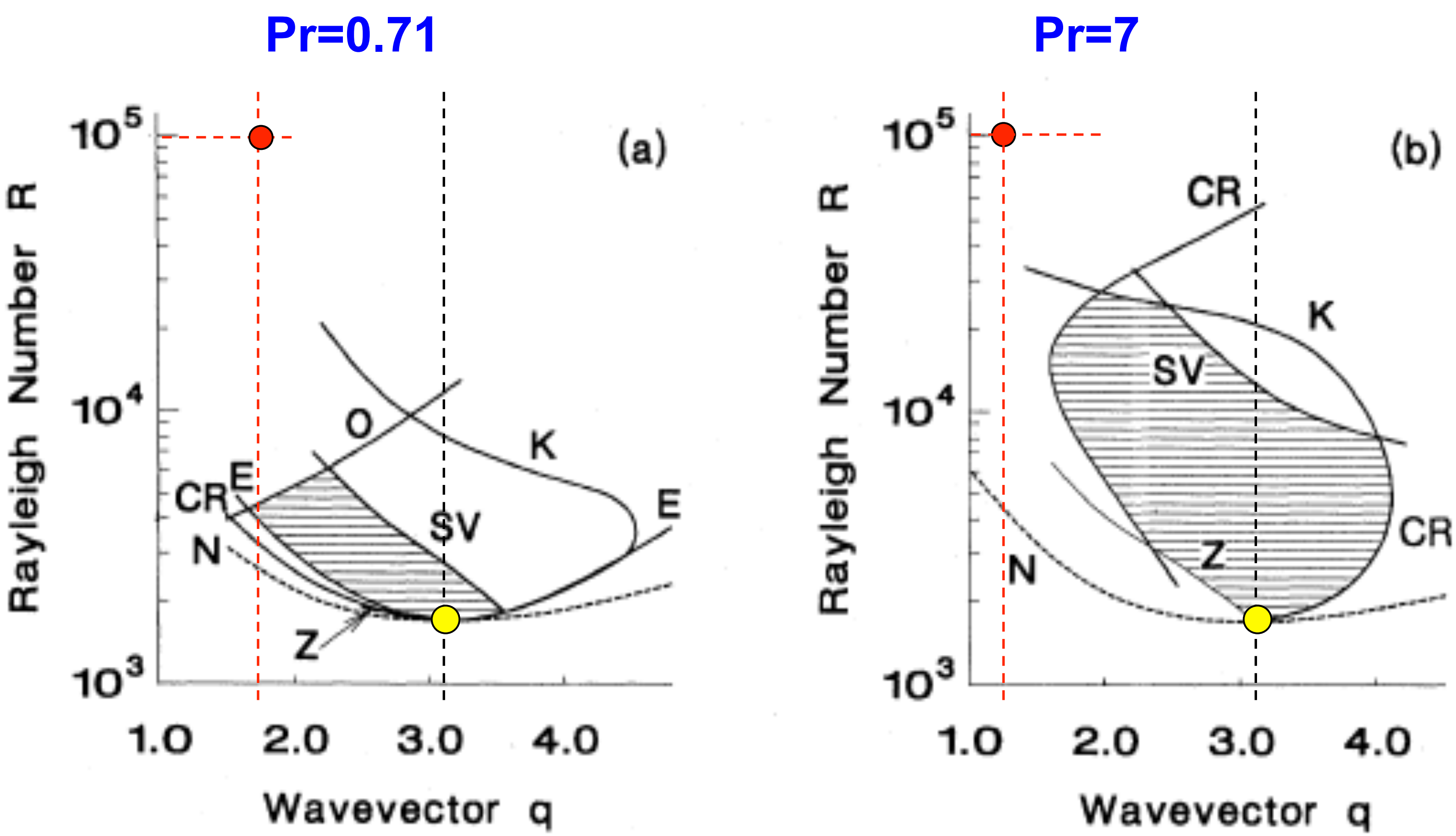


Knot or oscillating instability

Knot or cross-roll instability

# Connection to boundary layer dynamics

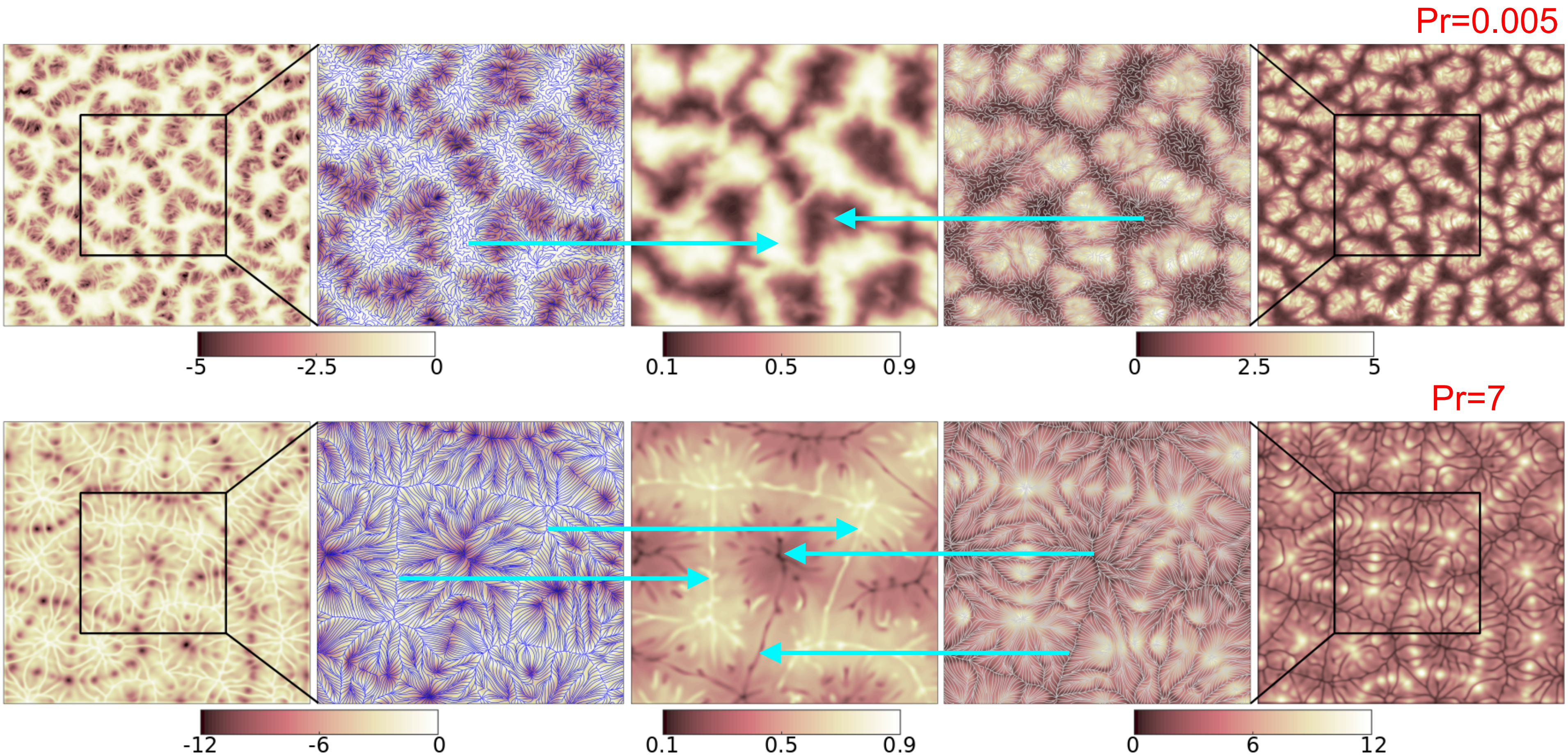


| Bottom Plate | Bottom Plate (zoom) | Midplane (zoom) | Top Plate (zoom) | Top Plate |
|---|---|---|---|---|
| $\frac{\partial T}{\partial z}\Big\|_{z=0}$ | $\vec{s} = \left(\frac{\partial u_x}{\partial z}\Big\|_{z=0}, \frac{\partial u_y}{\partial z}\Big\|_{z=0}\right)$ | $T\Big\|_{z=\frac{1}{2}}$ | $\vec{s} = \left(\frac{\partial u_x}{\partial z}\Big\|_{z=1}, \frac{\partial u_y}{\partial z}\Big\|_{z=1}\right)$ | $-\frac{\partial T}{\partial z}\Big\|_{z=1}$ |

# Skin friction field as a blueprint for plume formation

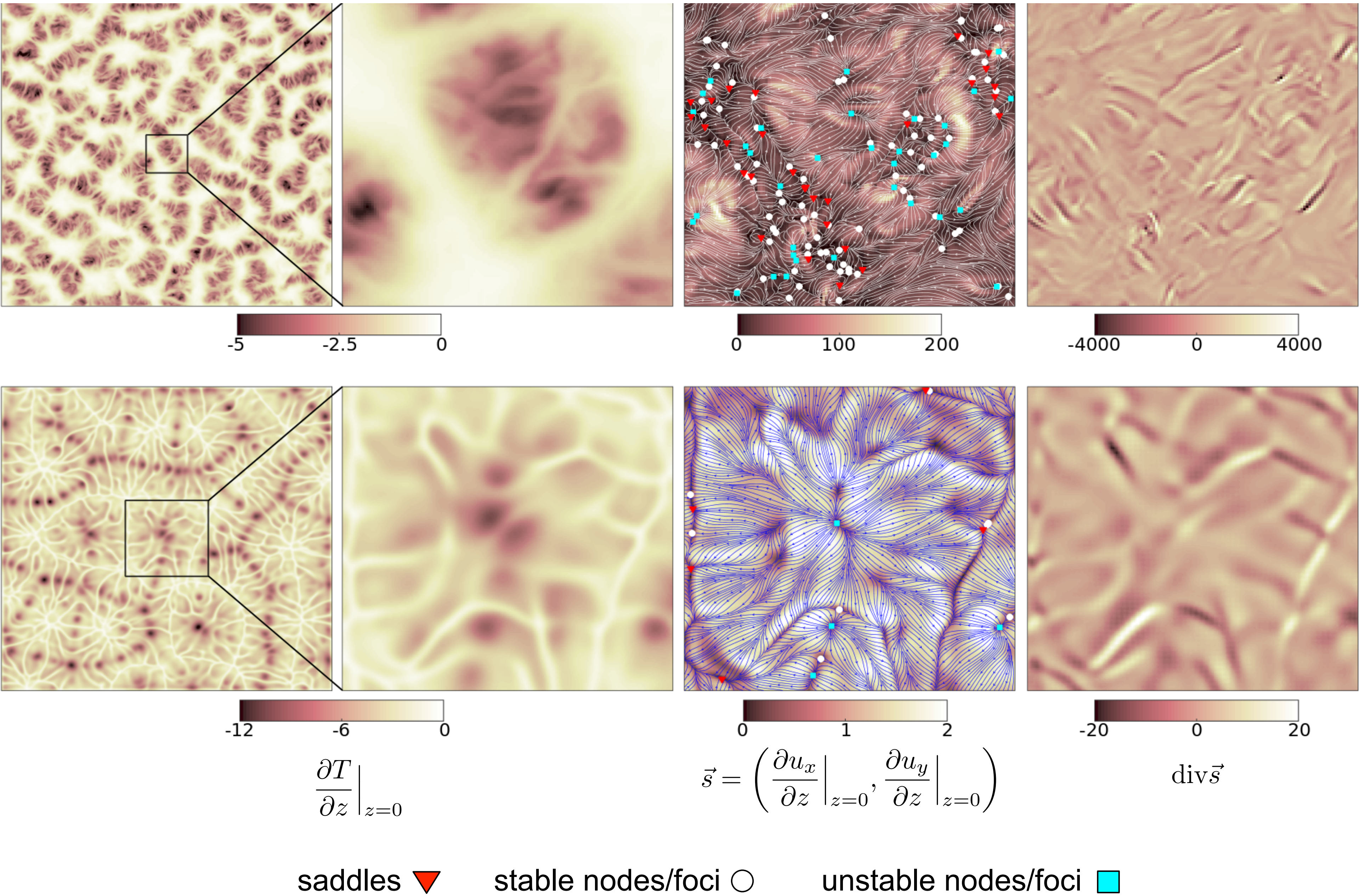

# Comparison of azimuthal spectra

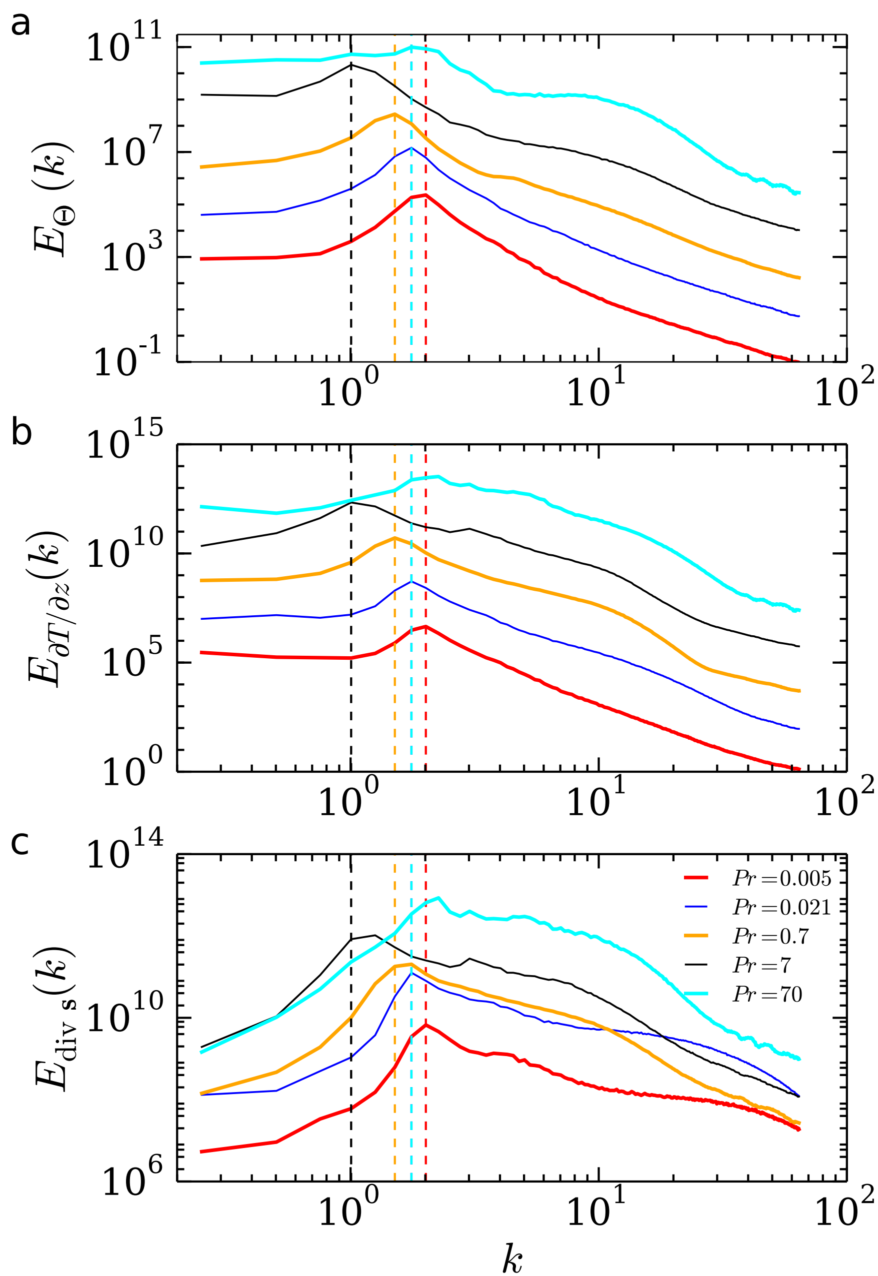


Peak wavenumbers of all three time-averaged spectra do agree

Midplane

Top and bottom plates

# Defects of superstructure patterns

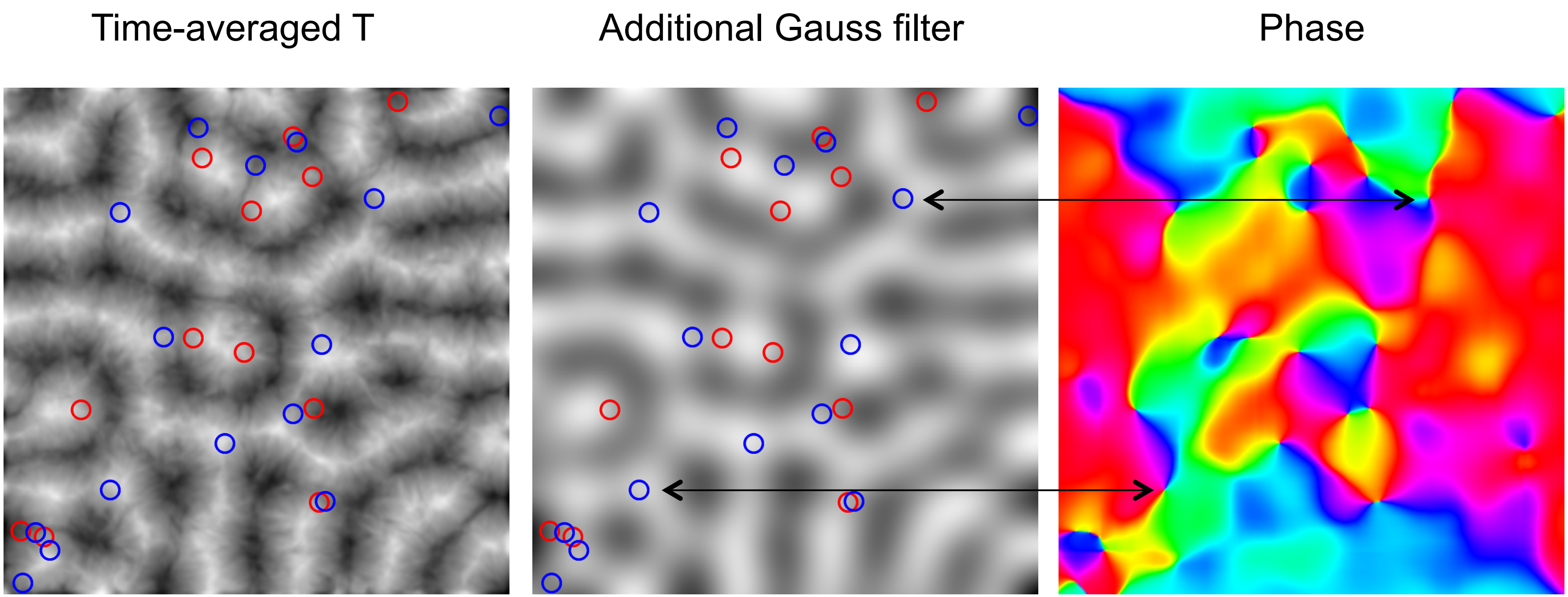


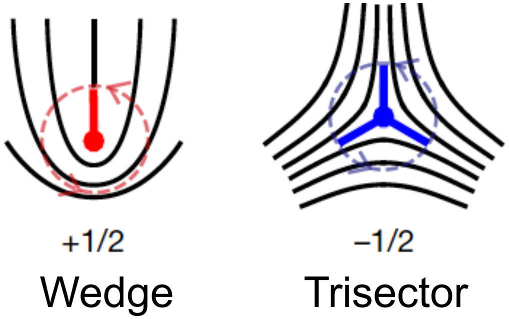


$$\phi = \frac{1}{2} \arctan \frac{2I_{xy}}{I_{xx} - I_{yy}}$$

Topological points defects detectable in superstructure patterns

# Circulation rolls

*Ender, Weiss, Pandey, JS & Westermann, submitted to Eurographics 2018*

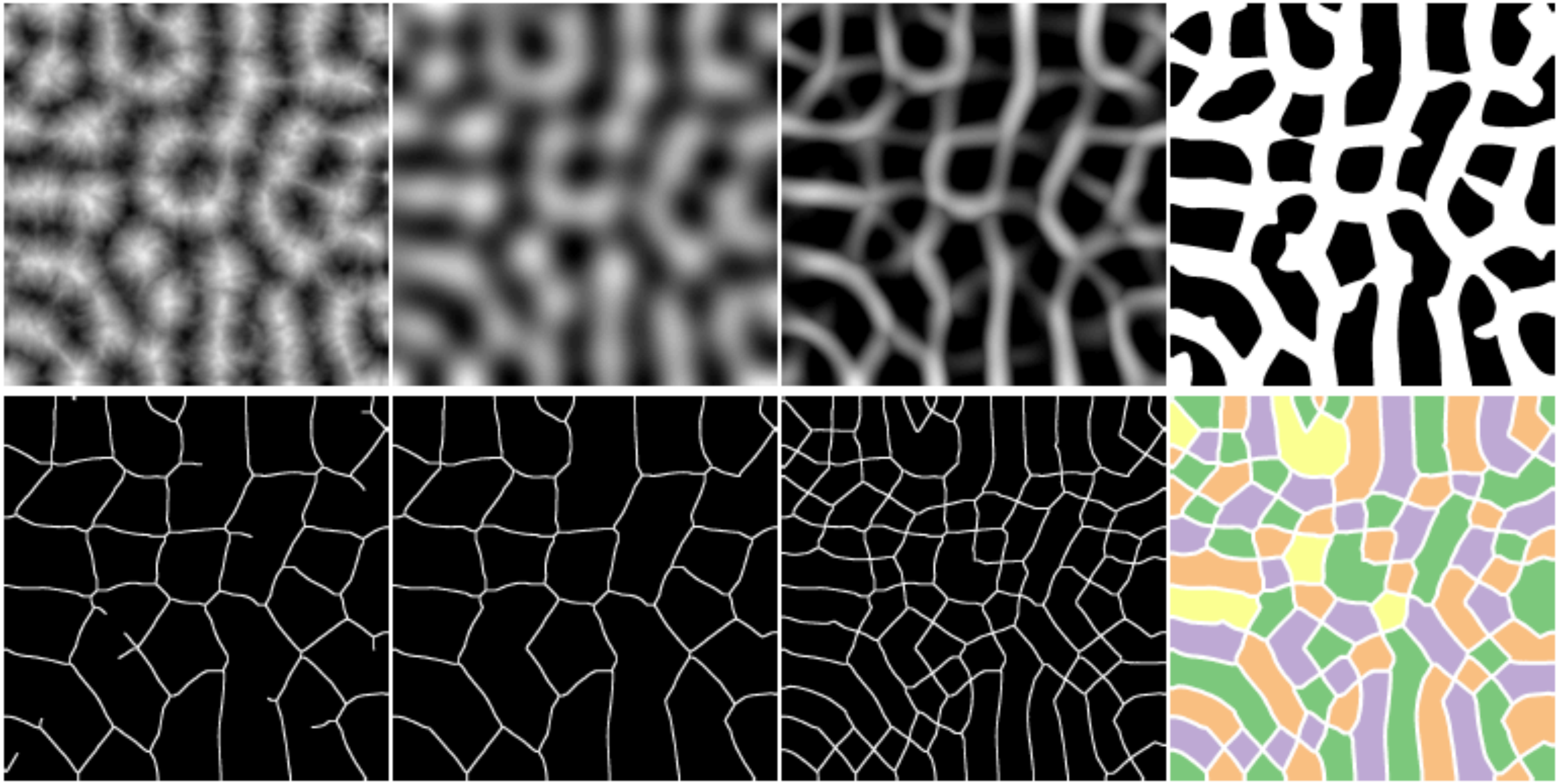

Separation of different circulation rolls segments on the basis of T to study mixing and transport on long time scales

# Lagrangian analysis of superstructures

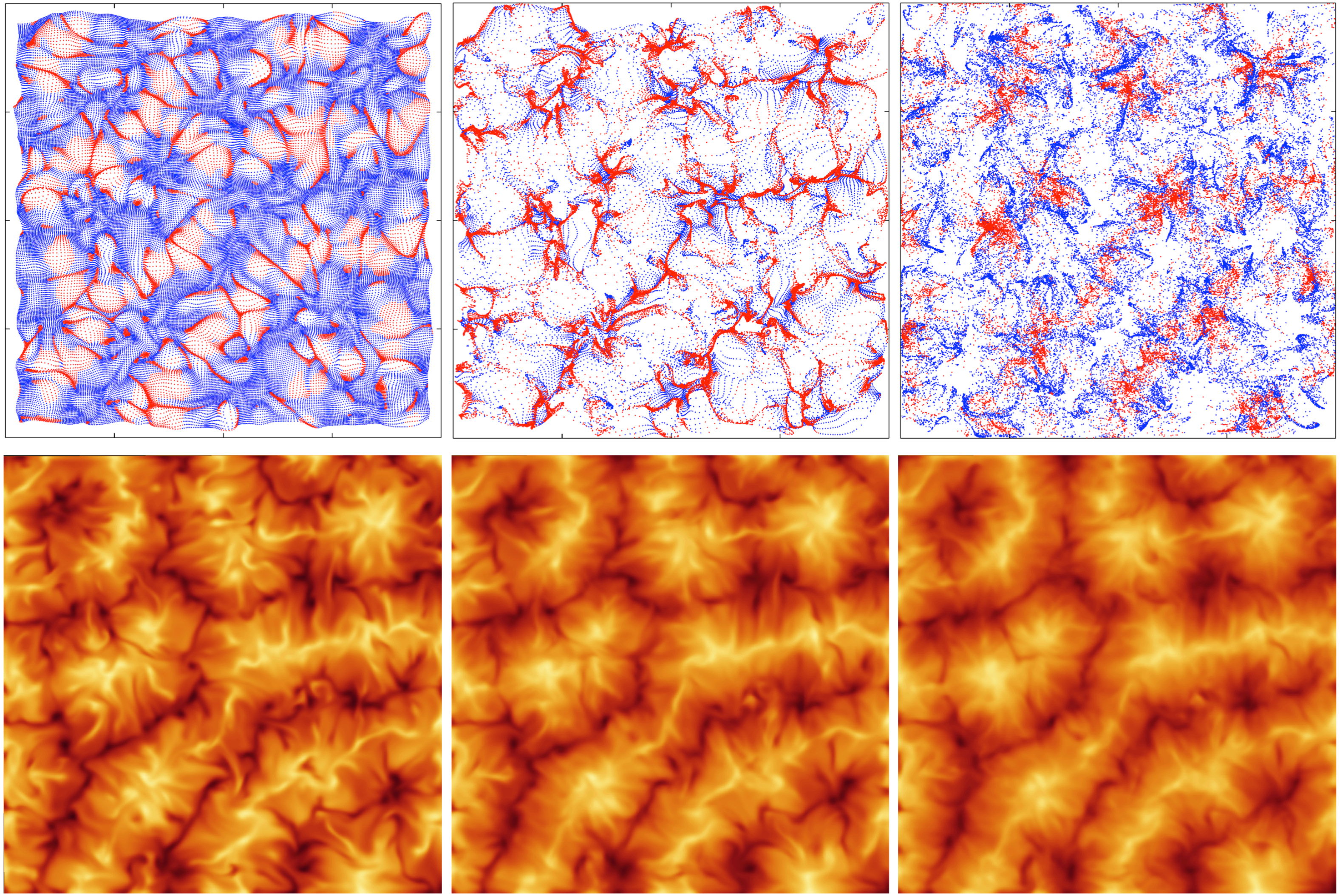

From single tracers & pairs to tracer clusters in extended domains

# Approach by graph theory

*Shi & Malik, IEEE Trans. Patt. Anal. Machine Intell. 2000*

- Lagrangian tracer ensemble is composed to a space-time graph
- Superstructure detection = Image segmentation = Balanced cut problem for a graph

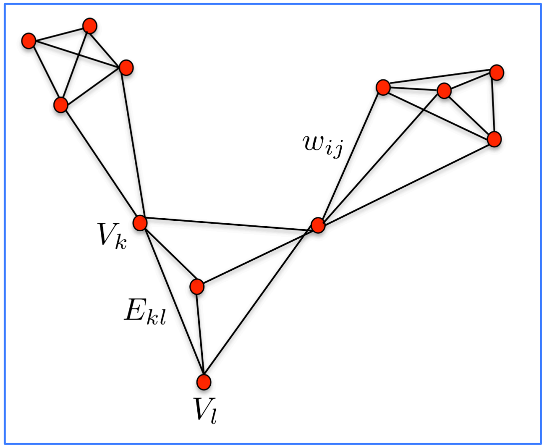


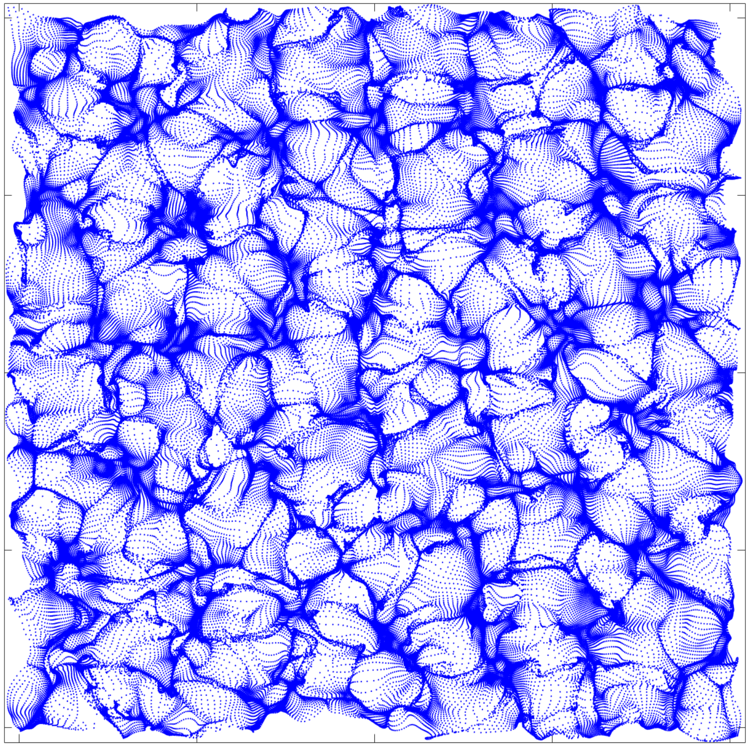

- $G = \{V, E, W\}$
- $r_{ij}(t_1) = \frac{1}{t_1} \int_0^{t_1} |\vec{x}_i(t) - \vec{x}_j(t)|\, dt$
- $w_{ij} = \begin{cases} K \gg 1 & : \quad i = j \\ \frac{1}{r_{ij}} & : \quad i \neq j \end{cases}$
- $L\vec{y} = \lambda D\vec{y} \quad \longrightarrow \quad D^{-1/2} L D^{-1/2} \vec{z} = \lambda \vec{z}$

# Cutting the graph into cluster

Eigenvalue spectrum of graph Laplacian

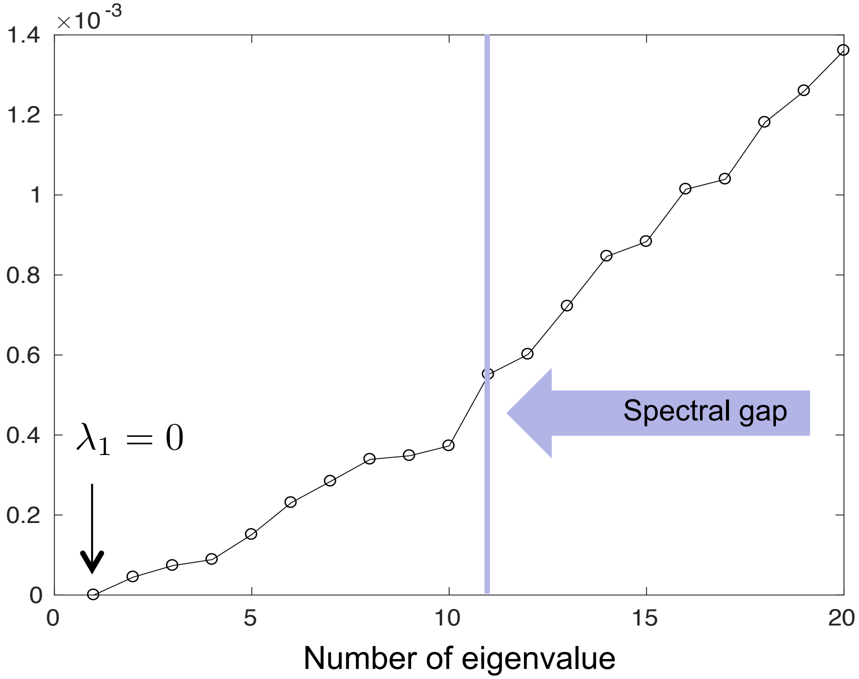


$$r_{ij} \leq \epsilon \Rightarrow w_{ij} = \frac{1}{r_{ij}} \quad r_{ij} > \epsilon \Rightarrow w_{ij} = 0$$

Clusters from spectral analysis of graph Laplacian agree with superstructures

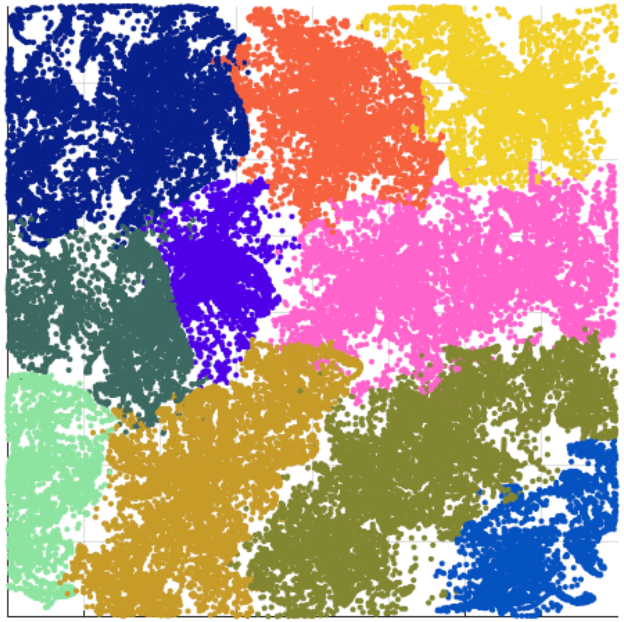

11 spectral clusters

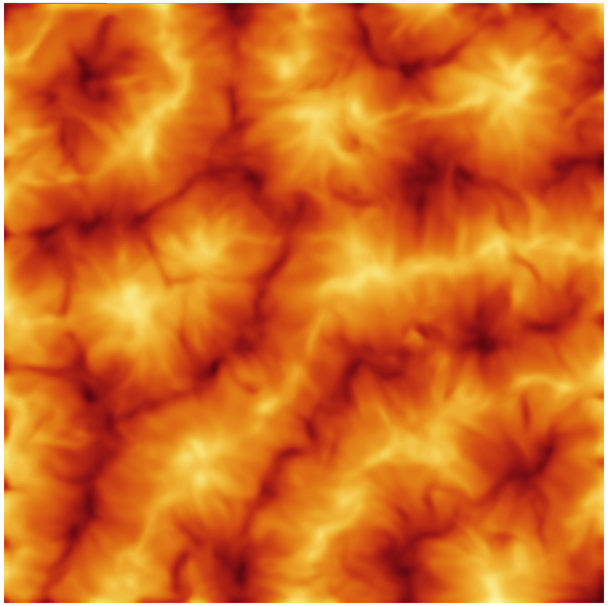

Time-averaged temperature in midplane

# Finding the right cutoff scale ε

*Scheel & JS, J. Fluid Mech. 2014*

$$r_{ij} \leq \epsilon \Rightarrow w_{ij} = \frac{1}{r_{ij}} \qquad r_{ij} > \epsilon \Rightarrow w_{ij} = 0$$

Local thermal boundary layer thickness ⟺ Characteristic superstructure scale

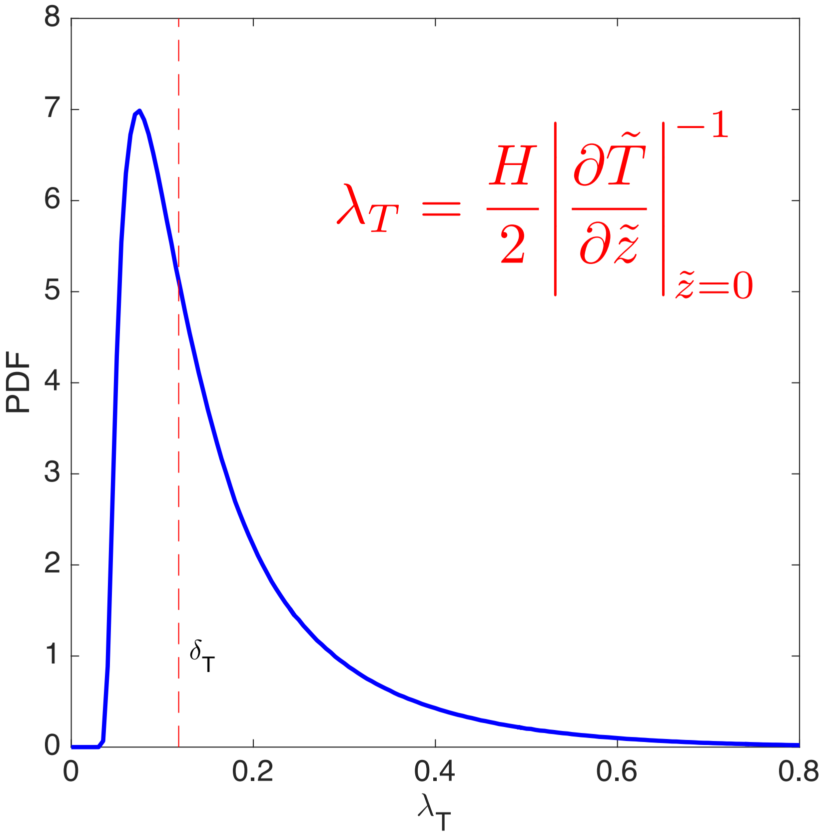


$$\lambda_T = \frac{H}{2}\left|\frac{\partial \tilde{T}}{\partial \tilde{z}}\right|^{-1}_{\tilde{z}=0}$$

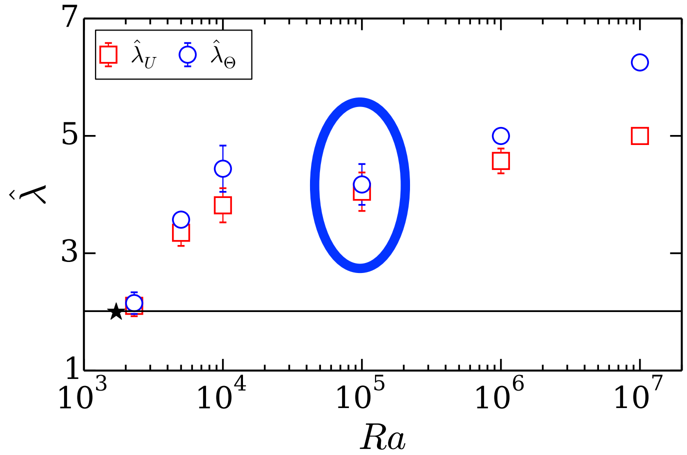


$$\lambda_\Theta \approx 2$$

# Summary

- Large-scale patterns are detected in turbulent RBC for all Ra and Pr once the fast small-scale fluctuations are removed
- Characteristic mean pattern scale depends on Pr and Ra in present parameter range
- Patterns evolve gradually on time scales that are significantly larger than the free-fall time, but significantly smaller than diffusion time
- Pattern scales are correlated to characteristic scale of skin friction field at plates and thus to formation of plume ridges
- Changes of superstructure patterns are associated with the generation and annihilation of topological point defects
- Spectral analysis of graph Laplacian reveals superstructure pattern scales in Lagrangian frame

NIC
GCS Gauss Centre for Supercomputing
lrz Leibniz-Rechenzentrum der Bayerischen Akademie der Wissenschaften
DFG Turbulent Superstructures

http://lanl.arxiv.org/abs/1801.04478